


Systematic analysis of flow distributions

Hadi Mehrabpour ^{*}

School of Particles and Accelerators, Institute for Research in Fundamental Sciences (IPM), P. O. Box 19395-5531, Tehran, Iran and Frankfurt Institute for Advanced Studies, Giersch Science Center, D-60438 Frankfurt am Main, Germany



(Received 2 July 2020; revised 10 September 2020; accepted 9 October 2020; published 11 December 2020)

The information of the event-by-event fluctuations are extracted from flow harmonic distributions and cumulants, which can be done experimentally. In this work, I employ the standard method of Gram-Charlier series with normal kernel to find such distribution, which is the generalization of recently introduced flow distributions for the studies of the event-by-event fluctuations. In this path, I find the shifted cumulants $j_n\{2k\}$ which consist of the collision geometry information. The experimental data imply that not only all of the information about the event-by-event fluctuations of collision zone properties and different stages of heavy-ion process are not encoded in the radial flow distribution $p(v_n)$, but also the observables describing harmonic flows can generally be given by the joint distribution $\mathcal{P}(v_1, v_2, \dots)$. In such way, I first introduce a set of joint cumulants \mathcal{K}_{nm} , and then I find the flow joint distribution using these joint cumulants. Finally, I show that the symmetric cumulants SC(2, 3) and SC(2, 4) obtained from ALICE data are explained by the combinations $\mathcal{K}_{22} + \frac{1}{2}\mathcal{K}_{04} - \mathcal{K}_{31}$ and $\mathcal{K}_{22} + 4\mathcal{K}_{11}^2$.

DOI: [10.1103/PhysRevC.102.064907](https://doi.org/10.1103/PhysRevC.102.064907)

I. INTRODUCTION

The collective behavior of the initial fireball, which is created in heavy-ion collisions, can be experimentally measured by anisotropic flow. Anisotropic flow is traditionally quantified with harmonics v_n , the coefficients of the momentum distribution Fourier expansion in the azimuthal direction, which have been measured by the several experimental groups at Relativistic Heavy Ion Collider and Large Hadron Collider [1–8]. Due to the randomness of reaction plane angle and low statistic at each event, anisotropic flow finding is experimentally challenging. There are several techniques to solve these problems [9–13]. One of them is 2k-particle correlation functions $c_n\{2k\}$ (radial cumulants) [12,13]. On the other hand, the experimental results show that the flow harmonics fluctuate event by event even if a specific centrality class is considered [14,15]. The flow fluctuations contain the information of the collision geometry, quantum fluctuations at initial state, and effects of different evolution stages in heavy-ion process [16,17]. The distribution of flow harmonic not only can solve the problems of the reaction plane angle effect and low statistic in a given event but also can help us extract the information of observed event-by-event fluctuations. So these issues motivate us to study the radial flow distributions $p(v_n)$.

Experimentally flow distributions for second, third, and fourth harmonics have been obtained using the unfolding method [18,19]. Also it has been found that the Bessel-Gaussian distribution describe the observed flow distributions in some centrality collisions [19–21].

It should be noted that the information of flow fluctuations not only are encoded in the flow harmonic distribution $p(v_n)$, but also this information can be extracted from ra-

dial cumulants $c_n\{2k\}$ [22,23]. Consequently, finding a right set of cumulants and connecting them to flow harmonic distribution $p(v_n)$ can help us get closer to an exact interpretation of the event-by-event fluctuations. Thereby, different distributions and their cumulants have recently been introduced and investigated to explain the contributions of all evolution stages on the fluctuations. In Ref. [22], odd flow harmonic distributions have been obtained by employing two-dimensional (2D) standardized cumulants. In addition, using Gram-Charlier, a series with orthogonal polynomials, $p_{\text{odd}}(v_n)$ has been found in Ref. [23]. The experimental data of the even flow harmonics cannot be explained by the Bessel-Gaussian distribution in peripheral collisions. So finding the corrections to the Bessel-Gaussian distribution is crucial. Reference [23] considered an ansatz series as the corrections to the Bessel-Gaussian distribution. They employed moments to find the corresponding coefficients of this series. Their suggested flow distribution could decently explain both even and odd harmonics.

Experiments show that the event-plane correlations and event-by-event correlations of flow magnitudes are nonvanishing [25–27]. Thus, all of the information about the fluctuations can be extracted from a joint flow distribution $\mathcal{P}(v_1, v_2, \dots)$, which can explain the correlations between flow harmonics, event-by-event initial fluctuations, and correlations between different stages in heavy-ion collision processes. Now a question arises: Is there an unambiguous technique to find such radial flow distributions $p(v_n)$? Furthermore, can one find a joint flow distribution to interpret the most general form of the event-by-event fluctuations? The purpose of this paper is the answer to this question by introducing a systematic analysis of flow fluctuations so that one can find the cumulant coefficients and the consequently flow harmonic distributions.

In this work, I employ the standard method of Gram-Charlier series with normal kernel to introduce this analysis

^{*}hadi.mehrabpour.hm@gmail.com

in Sec. II. I also show that, using this technique, one can find the radial cumulants $c_n\{2k\}$ to flow moments $\langle v_n^{2k} \rangle$. In Sec. III, expanding the relation between moment and cumulant characteristic functions to two dimensions, I first rederive the relations between $\langle v_n^{2k} \rangle$ and $c_n\{2k\}$, and then I find the distribution of odd flow harmonics which has been found in Refs. [22] and [23]. After that, I find a general form of flow distribution which is true for both even and odd harmonics. On the way to finding this distribution, I first find the shifted cumulants $j_n\{2k\}$ which consist of the collision geometry information, and then, using the standard method of finding Gram-Charlier series, I obtain the flow distribution. It is worth mentioning that in order to show how much the flow distribution is a good approximation, I need to have a sample for $p(v_n)$. To this end, I generate heavy-ion collision events by employing a hydrodynamic based event generator which is called iEBE-VISHNU. The iEBE-VISHNU builds up a general theoretical framework for model-data comparisons through large scale Monte-Carlo simulations. The iEBE-VISHNU code package performs event-by-event simulations for relativistic heavy-ion collisions using viscous hydrodynamics + hadronic cascade model [24]. In the final step, I introduce a joint distribution of flow harmonics and its cumulants \mathcal{K}_{nm} in Sec. IV. I conclude Sec. IV by showing ALICE data can be described the combinations of joint cumulants. Moreover, the simulation data can be explained by the obtained joint distribution of flow harmonics. I present the conclusion in Sec. V.

II. SYSTEMATIC TECHNIQUE

Azimuthal asymmetry of the final-state single-particle distribution,

$$\frac{dN}{d\phi} = \frac{1}{2\pi} \sum_{n=-\infty}^{\infty} V_n e^{-in\phi}, \quad (1)$$

is quantified by the complex anisotropic flow coefficients (or flow vector) $V_n \equiv v_n e^{in\psi_n} = \{e^{in\phi}\}$, where ϕ is the azimuthal direction of an emitted particle, v_n is the amplitude of anisotropic flow in the n th harmonic, and ψ_n is the corresponding symmetry plane. Anisotropic flow, which is the hydrodynamic response to the anisotropic initial density profile, is one of the most important observables in characterizing the properties of QGP evolution. Flow fluctuates event by event, because it is stochastic and fluctuations are unavoidable. It is worth mentioning that the flow event-by-event fluctuations are a reflection of the initial-state fluctuations such that it is sensitive to details of initial geometry and its fluctuations. All of these lead us to search for the underlying probability density function (p.d.f.) of flow fluctuations. Hence, presenting a general method to find the flow distribution and its cumulants to explain the event-by-event flow fluctuations becomes important. In this section, I introduce such a method using the relation between the moment- and cumulant-generating functions. For simplicity I consider one-dimensional generating functions. In statistics, the generating function of moments in one dimension is $G(t) = \int dx e^{itx} p(x) \equiv \langle e^{itx} \rangle$. Also, the cumulant-generating

function is defined as the logarithm of the characteristic function, $K(t) \equiv \ln \langle e^{itx} \rangle = \sum_{n=1}^{\infty} \frac{(it)^n}{n!} \kappa_n$, which implies $G(t) = \exp[\sum_{n=1}^{\infty} \frac{(it)^n}{n!} \kappa_n]$ [28–30]. Note that κ_n is the n th cumulants. Furthermore, the relation between cumulants and moments by using definitions of $G(t)$ and $K(t)$ is

$$1 + \sum_{n=1}^{\infty} \frac{\mu_n (it)^n}{n!} = \exp \left[\sum_{n=1}^{\infty} \frac{\kappa_n (it)^n}{n!} \right], \quad (2)$$

where $\mu_n = \langle x^n \rangle$. The relation between n th moment and cumulants can be obtained by differentiating both sides of Eq. (2) n times and evaluating the result at $t = 0$,

$$K^{(n)}(t)|_{t=0} = (\log G(t))^{(n)}|_{t=0}. \quad (3)$$

Let us expand $G(t)$ in Eq. (2) to second order and set $\kappa_1 = \mu_1 \equiv \mu$ and $\kappa_2 = \sigma^2$. The structure of the generating function thus becomes the following:

$$\begin{aligned} G(t) &= \exp \left[\sum_{n=3}^{\infty} \kappa_n \frac{(it)^n}{n!} + \kappa_1 (it) + \kappa_2 \frac{(it)^2}{2!} \right] \\ &= \exp \left[\sum_{n=3}^{\infty} \kappa_n \frac{(it)^n}{n!} \right] e^{it\mu - \frac{t^2\sigma^2}{2}}, \\ &\equiv \exp \left[\sum_{n=3}^{\infty} \kappa_n \frac{(it)^n}{n!} \right] G_N(t), \end{aligned} \quad (4)$$

with $G_N(t) \equiv \exp[it\mu - \frac{t^2\sigma^2}{2}]$. Note that integrating by parts gives $(it)^n G_N(t)$ as the characteristic function of $(-D)^n G_N(x)$, where D is the differential operator [31]. On the other hand, one can find the probability density function $p(x)$ by using the last line of the defined moment-generating function in Eq. (4):

$$\begin{aligned} p(x) &= \frac{1}{2\pi} \int dt e^{-itx} G(t) \\ &\approx \frac{e^{-\frac{(x-\mu)^2}{2\sigma^2}}}{\sqrt{2\pi}\sigma} \left[1 + \sum_{n=3}^{\infty} \frac{\kappa_n}{n!\sigma^n} H_{e_n} \left(\frac{x-\mu}{\sigma} \right) \right], \end{aligned} \quad (5)$$

where H_{e_n} is the probabilists' Hermite polynomials,

$$H_{e_n}(x) = (-1)^n e^{\frac{x^2}{2}} \frac{d^n}{dx^n} e^{-\frac{x^2}{2}}. \quad (6)$$

This technique is the standard method of finding Gram-Charlier series with the normal kernel [32]. In this method, one can find the p.d.f. without any considered ansatz for the p.d.f.

To see how this method can help us to find the distribution of flow harmonics and cumulants, I first define the form of characteristic function using Eq. (2) as follows:

$$G(\lambda) = \langle e^{i v \cdot \lambda} \rangle = \langle e^{i v_n \lambda \cos(\Psi_n - \Psi_n)} \rangle, \quad (7)$$

where I have used the notation $\Psi_n = n\psi_n$. Since a one-dimensional characteristic function is needed to find the relations between cumulants and moments in the case of flow harmonics, one can integrate over Ψ_n to have $G(\lambda)$ [23],

$$G(\lambda) = \langle J_0(\lambda v_n) \rangle. \quad (8)$$

So the relation between the generating functions of $2k$ -particle cumulants $c_n\{2k\}$ [12,13] and flow magnitude moments $\langle v_n^{2k} \rangle$

are

$$\begin{aligned} \langle J_0(\lambda v_n) \rangle &= 1 + \left[\sum_{k=1}^{\infty} \frac{(-1)^k \lambda^{2k} \langle v_n^{2k} \rangle}{4^k (k!)^2} \right] \\ &= \exp \left[\sum_{k=1}^{\infty} \frac{i^{2k} c_n\{2k\} \lambda^{2k}}{4^k (k!)^2} \right], \end{aligned} \quad (9)$$

where J_ν is the Bessel functions of the first kind,

$$J_\nu(x) = \sum_{k=0}^{\infty} \frac{(-1)^k}{k! \Gamma(k + \nu + 1)} \left(\frac{x}{2} \right)^{2k + \nu}. \quad (10)$$

In the results, $2k$ -particle cumulants $c_n\{2k\}$ can be given to the measured v_n at each event by differentiating both sides of Eq. (9) at $\lambda = 0$:

$$\begin{aligned} c_n\{2\} &= \langle v_n^2 \rangle, \\ c_n\{4\} &= \langle v_n^4 \rangle - 2\langle v_n^2 \rangle^2, \\ c_n\{6\} &= 12\langle v_n^2 \rangle^3 - 9\langle v_n^4 \rangle \langle v_n^2 \rangle + \langle v_n^6 \rangle, \\ c_n\{8\} &= -144\langle v_n^2 \rangle^4 + 144\langle v_n^4 \rangle \langle v_n^2 \rangle^2 \\ &\quad - 16\langle v_n^6 \rangle \langle v_n^2 \rangle - 18\langle v_n^4 \rangle^2 + \langle v_n^8 \rangle, \\ &\vdots \end{aligned} \quad (11)$$

As can be seen in Eq. (11), the odd moment of radial flow distribution are absent in the definitions of $c_n\{2k\}$. So one can conclude that the radial flow distribution has more information than $2k$ -particle correlation functions. Finding the flow distribution is left to the next section.

So far I have presented a well-known technique in statistic theory to find the probability distribution and its cumulants. As can be seen, using this technique one could find the $2k$ -particle cumulants. In the following I first obtain the flow distribution of odd harmonics [22]. Then I try to find a general probability distribution to explain the event-by-event fluctuation which is true for both odd and even flow harmonics.

III. TWO-DIMENSIONAL CUMULANT AND MOMENT RELATIONS

As mentioned, introducing a method to find flow harmonic distribution that extract the maximum amount of information is necessary. Here I present a technique commonly used in statistics to achieve this goal. To find the relations between moments and cumulants of flow harmonics, I use the joint generating functions [33],

$$\log \langle e^{\lambda z + \lambda^* z^*} \rangle = \sum_{k,l} \frac{\lambda^{*k} \lambda^l}{k! l!} \kappa\{k, l\}, \quad (12)$$

where $\kappa\{k, l\}$ are joint cumulants. It is worth emphasizing that Eq. (12) is a general formula. Moreover, to find the desired flow distributions one needs to modify Eq. (12) by choosing different definitions of z and λ .

In Ref. [22], an expansion of flow distribution for odd harmonics has been found (also see Eq. (24) in Ref. [23]). To reproduce this expansion, I have to set $z \equiv v_n$ and $\lambda \equiv$

$(\lambda_x - i\lambda_y)/2$ in Eq. (12). By replacing these considerations in Eq. (12), I arrive at

$$\langle e^{v_{n,x} \lambda_x + v_{n,y} \lambda_y} \rangle = \exp \left[\sum_{kl} \frac{(\lambda_x + i\lambda_y)^k (\lambda_x - i\lambda_y)^l}{2^{(k+l)} k! l!} c_n\{k, l\} \right]. \quad (13)$$

Here I use the common notation of c_n for $2k$ -particle cumulants. Note that in Eq. (13) only terms with $k = l$ are nonzero. Also, setting $k = l$ the relations in Eq. (11) are reproduced [34]. The cumulant $c_n\{k, k\} \equiv c_n\{2k\}$ can be obtained by differentiating both sides of Eq. (12),

$$\begin{aligned} &\frac{\partial^{2k}}{\partial \lambda_x^k \partial \lambda_y^k} \left\{ \langle e^{v_{n,x} \lambda_x + v_{n,y} \lambda_y} \rangle \right\} \\ &= \exp \left[\sum_{kl} \frac{(\lambda_x + i\lambda_y)^k (\lambda_x - i\lambda_y)^k}{4^k (k!)^2} c_n\{2k\} \right], \end{aligned} \quad (14)$$

and evaluating the results at $\lambda_x = 0$ and $\lambda_y = 0$. To find the odd flow distributions [35], I use the first line of Eq. (5) [36] and the Fourier transformation of characteristic function, $\lambda_x^2 + \lambda_y^2 \rightarrow \partial_x^2 + \partial_y^2$. The probability distribution for odd harmonics thus becomes (see Appendix A)

$$\begin{aligned} &p_{\text{odd}}(v_{n,x}, v_{n,y}) \\ &= \exp \left[\sum_{k=2} c_n\{2k\} \frac{(\partial_x^2 + \partial_y^2)^k}{2^{2k} (k!)^2} \right] \left[\frac{1}{\pi c_n\{2\}} e^{-\frac{v_{n,x}^2 - v_{n,y}^2}{c_n\{2\}}} \right]. \end{aligned} \quad (15)$$

Rewriting this distribution in polar coordinates, $v_n^2 = v_{n,x}^2 + v_{n,y}^2$, one can obtain the radial odd flow distribution,

$$\begin{aligned} &\int dv_{n,x} dv_{n,y} p_{\text{odd}}(v_{n,x}, v_{n,y}) \\ &= \int \frac{v_n dv_n d\Psi_n}{\pi c_n\{2\}} \exp \left[\sum_{k=2} \frac{c_n\{2k\} \mathbf{D}_{v_n, \Psi_n}^k}{4^k (k!)^2} \right] e^{-\frac{v_n^2}{c_n\{2\}}} \\ &= \int dv_n p_{\text{odd}}(v_n), \end{aligned} \quad (16)$$

where $\mathbf{D}_{v, \Psi}$ represent $\mathbf{D}_v + (1/v^2) \partial_\Psi^2$ and \mathbf{D}_v is $\partial_v^2 + (1/v) \partial_v$. Therefore, the radial distribution of odd flow harmonics $p_{\text{odd}}(v_n)$ is

$$p_{\text{odd}}(v_n) = \frac{2v_n}{c_n\{2\}} \exp \left[\sum_{k=2} \frac{c_n\{2k\} \mathbf{D}_{v_n, \Psi_n}^k}{4^k (k!)^2} \right] e^{-\frac{v_n^2}{c_n\{2\}}}. \quad (17)$$

If the first exponential in Eq. (17) is expanded and truncated to the first order, the following relation is obtained:

$$p'_{\text{odd}}(v_n) = \frac{2v_n}{c_n\{2\}} \left[1 + \sum_{k=2} \frac{c_n\{2k\}}{4^k (k!)^2} \mathbf{D}_{v_n}^k \right] e^{-\frac{v_n^2}{c_n\{2\}}}. \quad (18)$$

The form of $p'_{\text{odd}}(v_n)$ can be found in terms of cumulants by evaluating the k th derivative of $\exp(-\frac{v_n^2}{c_n\{2\}})$ (see Appendix B) and letting $2\sigma^2 = c_n\{2\}$ for odd harmonics [22,23],

$$p'_{\text{odd}}(v_n) = \left(\frac{v_n}{\sigma^2} \right) e^{-\frac{v_n^2}{2\sigma^2}} \left\{ 1 + \sum_{k=2} \frac{(-1)^k \Gamma_{2k-2}^{\text{odd}}}{k!} L_k[v_n^2 / (2\sigma^2)] \right\}, \quad (19)$$

where $\Gamma_{2k-2}^{\text{odd}} = c_n\{2k\}/c_n\{2\}^k$ and L_k is the Laguerre polynomials,

$$L_k(x) = \sum_{n=0}^k \binom{k}{n} \frac{(-x)^n}{n!}. \quad (20)$$

The expansion (19) is exactly the flow distribution found in Ref. [22] which can explain any event-by-event flow fluctuations of odd harmonics.

Because $p_{\text{odd}}(v_{n,x}, v_{n,y})$ is rotationally symmetric ($\bar{v}_{2n+1} \equiv \langle v_{2n+1,x} \rangle = 0$) and consequently the main features of 2D and radial odd flow distribution are the same, obtaining distribution (19) is simple. But this case is not true for even flow harmonics, since $\bar{v}_{2n} \neq 0$. This is because even flow distributions are not rotationally symmetric, and reshuffling $(v_{n,x}, v_{n,y})$ leads to a partial loss of information of $p_{\text{even}}(v_{n,x}, v_{n,y})$. Hence, the main challenge is to find a radial flow distribution which can give a good approximation of flow fluctuations for even n so that the least amount of information is lost.

In the following, I begin to find the flow harmonic distribution and its cumulants by assuming nonzero \bar{v}_n . Modifying the relation (12) for even flow harmonics, the relation of moment- and cumulant-generating functions in 2D with $k = l$ can be rewritten as

$$\langle e^{(v_{n,x} - \bar{v}_n)\lambda_x + v_{n,y}\lambda_y} \rangle = \exp \left[\sum_k \frac{(\lambda_x^2 + \lambda_y^2)^k}{2^{2k}(k!)^2} j_n\{2k\} \right]. \quad (21)$$

where I consider $z \equiv V_n - \bar{v}_n$ and $\lambda \equiv \frac{\lambda_x - i\lambda_y}{2}$. I simply use the notation $W_n \equiv V_n - \bar{v}_n$ as a shifted flow vector so that $\langle W_n \rangle = 0$ [37]. The reason for choosing $k = l$ is to avoid obtaining complex j_n cumulants. By differentiating both sides of Eq. (21) at $\lambda_x = 0$ and $\lambda_y = 0$, one can find the relations between $j_n\{2k\}$ and moments,

$$\begin{aligned} j_n\{2\} &= \langle w_n^2 \rangle, \\ j_n\{4\} &= \langle w_n^4 \rangle - 2\langle w_n^2 \rangle^2, \\ j_n\{6\} &= \langle w_n^6 \rangle + 12\langle w_n^2 \rangle^3 - 9\langle w_n^2 \rangle \langle w_n^4 \rangle, \\ j_n\{8\} &= \langle w_n^8 \rangle - 144\langle w_n^2 \rangle^4 + 144\langle w_n^4 \rangle \langle w_n^2 \rangle^2 \\ &\quad - 16\langle w_n^6 \rangle \langle w_n^2 \rangle - 18\langle w_n^4 \rangle^2, \\ &\vdots \end{aligned} \quad (22)$$

where $w_n^2 = |W_n|^2 = (v_{n,x} - \bar{v}_n)^2 + v_{n,y}^2$. It is well known that the cumulants are invariant under shifting a random variable. For instance, the cumulant of a two-particle azimuthal correlation can be written as $\langle e^{in(\phi_1 - \phi_2)} \rangle - \langle e^{in\phi_1} \rangle \langle e^{-in\phi_2} \rangle$ for the case of a nonperfect detector [13]. If one shifts ϕ_1 and ϕ_2 by the same quantity $\phi_i \rightarrow \phi_i - \theta$, then the cumulant would stay invariant. In Eq. (22), $j_n\{2k\}$ are consist of some moments which are not invariant under shifting $\phi_i \rightarrow \phi_i - \theta$. Of course, one can find the cumulants $j_n\{2k\}$ are shift invariant by removing such moments. However, I renamed $j_n\{2k\}$ as ‘‘shifted cumulants’’ to avoid confusion. Also, it should be noticed that by choosing $\bar{v}_n = 0$, $2k$ -particle correlation functions $c_n\{2k\}$ can be recovered and $j_n\{2k\} = c_n\{2k\}$.

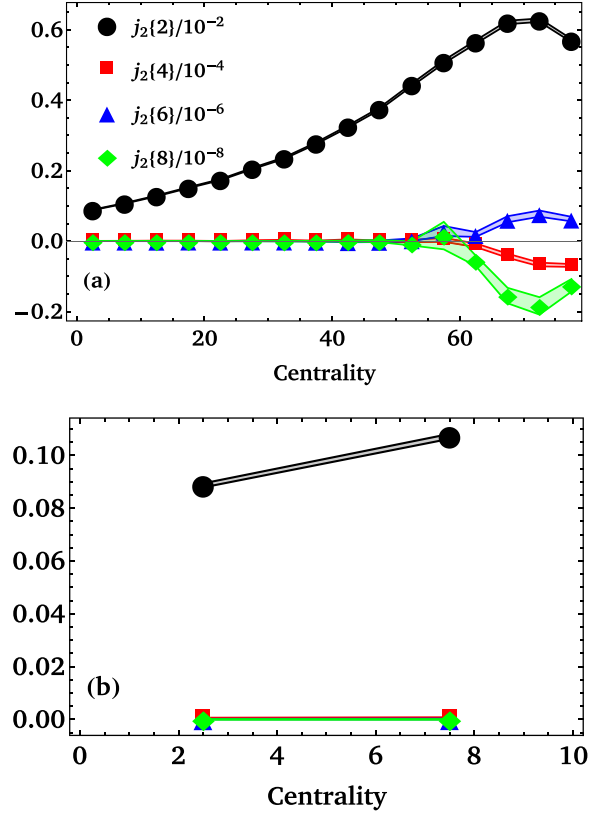


FIG. 1. Comparing the cumulants $j_2\{2k\}$ for $k = 2, 3$, and 4 obtained from the iEBE-VISHNU event generator. I separated results in two panels to compare the results in peripheral and most central collisions (0–5% and 5–10% centrality classes).

Figure 1 presents the cumulants $j_n\{2k\}$ for $n = 2$, obtained from the iEBE-VISHNU output and the comparisons between them. It should be mentioned that in the present work, I study the Pb-Pb collision with center-of-mass energy per nucleon pair $\sqrt{s_{NN}} = 2.76$ TeV. In this work, I use a Monte Carlo Glauber model for the initial state such that the wounded nucleon/binary collision mixing ratio was set to 0.118. The hydrodynamic starting time τ_0 was set to 0.6 fm/c, and $\eta/s = 0.08$ and zero balk viscosity are used for the hydrodynamic evolution. Note that the events generate in 16 centrality classes between 0 and 80% and I generated 14 000 events for each centrality. It should be emphasized that I have taken into account the charged hadrons π^\pm , K^\pm , p , and \bar{p} in the final particle distribution which are in the transverse momentum range $0.28 < p_T < 4$ GeV. In Fig. 1, I scaled shifted cumulants as $j_n\{2k\}/10^{-2k}$ to show $j_n\{4\}$, $j_n\{6\}$, and $j_n\{8\}$ in a plot. Also, I drew the shifted cumulants in the 0–5% and 5–10% centrality classes to compare the results of peripheral and most central collisions. As demonstrated in this figure, the differences between $j_n\{4\}$, $j_n\{6\}$, and $j_n\{8\}$ are sensible in peripheral central collisions such that the relation between $j_n\{2k\}$ is

$$j_n\{2\} \gg j_n\{4\} \gg j_n\{6\} \gg j_n\{8\} \gg \dots \quad (23)$$

Because the experimental results [7] show that $p_{\text{even}}(v_n)$ have a deviation from Bessel-Gaussian, this relation is expected. This deviation is more pronounced in peripheral collisions where the Bessel-Gaussian distribution cannot explain experimental data. Furthermore, one expects that the cumulants $j_n\{2k\}$ can quantify the main features of a distribution near Bessel-Gaussian. In Ref. [23], a new set of cumulants $q_n\{2k\}$ has been defined to study the distributions near Bessel-Gaussian. These cumulants also have been obtained from $2k$ -particle correlation functions $c_n\{2k\}$. Replacing the definitions of $q_n\{2k\}$ (see Eq. (36) in Ref. [23]) in Eq. (22), one can find

$$\begin{aligned} j_n\{2\} &= q_n\{2\}, \\ j_n\{4\} &= \frac{2}{7}(4q_n\{4\} + q_n\{2\}^2 + 40q_n\{2\}\bar{v}^2 + 16\bar{v}^4 \\ &\quad - 4\bar{v}(4\langle v_{n,x}^3 \rangle + 5\bar{v}\langle v_{n,y}^2 \rangle + 2\langle v_{n,x}v_{n,y}^2 \rangle) - 4\langle v_{n,x}^2 v_{n,y}^2 \rangle), \\ &\vdots \end{aligned} \quad (24)$$

such that $j_n\{2k\} = q_n\{2k\} + \dots$, for $k \geq 2$. A comparison between $j_n\{2k\}$ and $q_n\{2k\}$ obtained from iEBE-VISHNU are presented in Fig. 2. As can be seen, the difference between these sets of cumulants for $k \geq 2$ is significant, especially for midcentralities and peripheral collisions. This means that the amount of encoded information in these two sets are different. It should be noted the cumulant set $q_n\{2k\}$ has been defined by using the moments of the radial flow distribution $p_q(v_n; \bar{v}_n)$ in Ref. [23], but here I only used the relation between the joint cumulant- and moment-generating functions to find $j_n\{2k\}$. This means that my technique does not require any knowledge about the flow distributions.

The main challenge is finding the form of flow harmonic distributions by considering $\bar{v}_n \neq 0$. If one obtains the Fourier transformation of joint characteristic function of moments in Eq. (21), $\lambda_x \rightarrow -i\partial_x$ and $\lambda_y \rightarrow -i\partial_y$, then the 2D distribution $p(v_{n,x}, v_{n,y})$ [38] is obtained as

$$p(v_{n,x}, v_{n,y}) = \exp \left[\sum_{k=2} \frac{j_n\{2k\} \mathbf{D}^k}{4^k (k!)^2} \right] \mathcal{F}(v_{n,x}, v_{n,y}), \quad (25)$$

where \mathbf{D} is the differential operator with respect to λ_x and λ_y . Also, the distribution $\sqrt{2\pi} \sigma \mathcal{F}(v_{n,x}, v_{n,y})$ is a 2D Gaussian distribution with mean \bar{v}_n and standard deviation $\sqrt{j_n\{2\}}/2$. After some calculations in Cartesian coordinates, one gets

$$\mathbf{D}^k \mathcal{F}(v_{n,x}, v_{n,y}) = \frac{(-1)^k 4^k k!}{j_n\{2\}^k} \mathcal{F}(v_{n,x}, v_{n,y}) L_k \left(\frac{w_n^2}{j_n\{2\}} \right). \quad (26)$$

Since I follow the radial flow distribution, Eq. (26) can be written in polar coordinates as follows:

$$\begin{aligned} \mathbf{D}_{v_n, \Psi_n}^k \mathcal{F}(v_n; \bar{v}_n, \Psi_n) &= \frac{(-1)^k 4^k k!}{j_n\{2\}^k} \mathcal{F}(v_n; \bar{v}_n, \Psi_n) \\ &\quad \times \left[L_k \left(\frac{v_n^2 + \bar{v}_n^2}{j_n\{2\}} \right) + A_k + B_k \right], \end{aligned} \quad (27)$$

where the terms of A_k and B_k are

$$A_k = \alpha_k, \quad B_k = \sum_{l=1}^k \beta_{kl} \cos l\Psi_n. \quad (28)$$

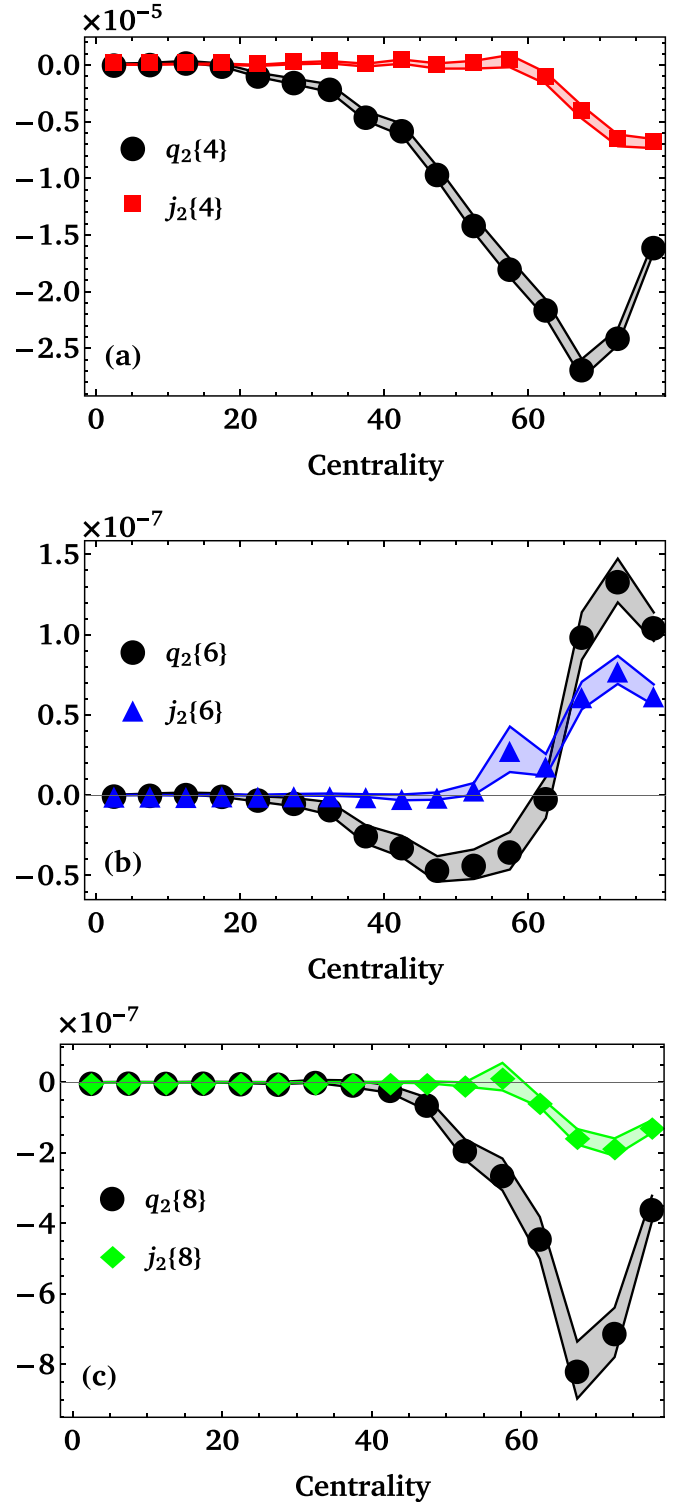


FIG. 2. Comparing the amount of information of cumulants $j_2\{2k\}$ and $q_2\{2k\}$ introduced in Ref. [23] as function of centrality.

The derivation of the n th derivative of $\mathcal{F}(v_{n,x}, v_{n,y})$ in Eq. (27) and definitions of the coefficients α and β are in the Appendix C. If I integrate “ $\mathcal{F}(v_n; \bar{v}_n, \Psi_n) \cos l\Psi_n$ ” over Ψ_n ,

then I arrive at

$$\begin{aligned}
& \int_0^\infty v_n dv_n \int_0^{2\pi} d\Psi \mathcal{F}(v_n; \bar{v}_n, \Psi_n) \cos l\Psi_n \\
&= \int_0^\infty dv_n \left(\frac{2v_n}{j_n\{2\}} \right) e^{-\frac{v_n^2 + \bar{v}_n^2}{j_n\{2\}}} I_l \left(\frac{2v_n \bar{v}_n}{j_n\{2\}} \right) \\
&= \int_0^\infty dr \mathcal{F}(v_n; \bar{v}_n) I_l \left(\frac{2v_n \bar{v}_n}{j_n\{2\}} \right). \quad (29)
\end{aligned}$$

Using Eq. (27), one gets

$$\begin{aligned}
& \int_0^\infty v_n dv_n \int_0^{2\pi} d\Psi_n \mathbf{D}_{v_n, \Psi_n}^k \mathcal{F}(v_n; \bar{v}_n, \Psi_n) \\
&= \int_0^\infty dv_n \frac{(-1)^k 4^k k!}{j_n\{2\}^k} \mathcal{F}(v_n; \bar{v}_n) \\
&\times \left\{ \left[L_k \left(\frac{v_n^2 + \bar{v}_n^2}{j_n\{2\}} \right) + \alpha_k \right] I_0 \left(\frac{2v_n \bar{v}_n}{j_n\{2\}} \right) \right. \\
&\left. + \sum_{l=1}^k \beta_{kl} I_l \left(\frac{2v_n \bar{v}_n}{j_n\{2\}} \right) \right\}. \quad (30)
\end{aligned}$$

The radial flow distribution $p(v_n; \bar{v}_n)$ using Eq. (30) can be obtained,

$$\begin{aligned}
p_q(v_n; \bar{v}_n) &= \int_0^{2\pi} d\Psi_n v_n p(v_n; \bar{v}_n, \Psi_n) \\
&\approx \int_0^{2\pi} d\Psi_n v_n \left[1 + \sum_{k=2}^q \frac{j_n\{2k\} \mathbf{D}_{v_n, \Psi_n}^k}{4^k (k!)^2} \right] \mathcal{F}(v_n; \bar{v}_n, \Psi_n) \\
&= \mathcal{F}(v_n; \bar{v}_n) \sum_{k=0}^q \frac{(-1)^k \gamma_k}{k!} \left[\alpha'_k I_0 \left(\frac{2v_n \bar{v}_n}{j_n\{2\}} \right) \right. \\
&\left. + \sum_{l=0}^k \beta_{kl} I_l \left(\frac{2v_n \bar{v}_n}{j_n\{2\}} \right) \right], \quad (31)
\end{aligned}$$

where $\alpha'_k \equiv L_k \left(\frac{v_n^2 + \bar{v}_n^2}{j_n\{2\}} \right) + \alpha_k$ and $\gamma_k \equiv j_n\{2k\} / j_n\{2\}^k = q_n\{2k\} / q_n\{2\}^k + \dots$. Note that I have assumed $\gamma_0 = 1$ and $\gamma_1 = \alpha_0 = \beta_{k0} = 0$ in Eq. (31). The first term ($q = 0$) of $p_q(v_n; \bar{v}_n)$ is a Bessel-Gaussian distribution. Other terms are the corrections to the Bessel-Gaussian distribution.

Figure 3 compares the obtained distribution from iEBE-VISHNU with estimated distribution in Eq. (31). In this figure, I investigate different truncations of $p_q(v_n; \bar{v}_n)$ for $q = 0, 2, 3, 4$ presented by dotted black, dashed red, dot-dashed blue, and solid green lines, respectively. Since the main shortcoming of the Bessel-Gaussian distribution compared with the simulation data are in peripheral collisions, I only show the results in 65–70%, 70–75%, and 75–80% centrality classes. As demonstrated in this figure, the generated data cannot be described by the black curve, which corresponds to the Bessel-Gaussian distribution. Also, studying χ^2/NDF for the Bessel-Gaussian distribution and $p_q(v_n; \bar{v}_n)$ for $q = 2, 3$, and 4 plotted in Fig. 4 for the investigated centralities in Fig. 3. As can be seen, the values of χ^2/NDF associated $p_q(v_n; \bar{v}_n)$ are more closer to 1 comparing with the Bessel-Gaussian distribution. The results of Fig. 3 and 4 show that the distribution

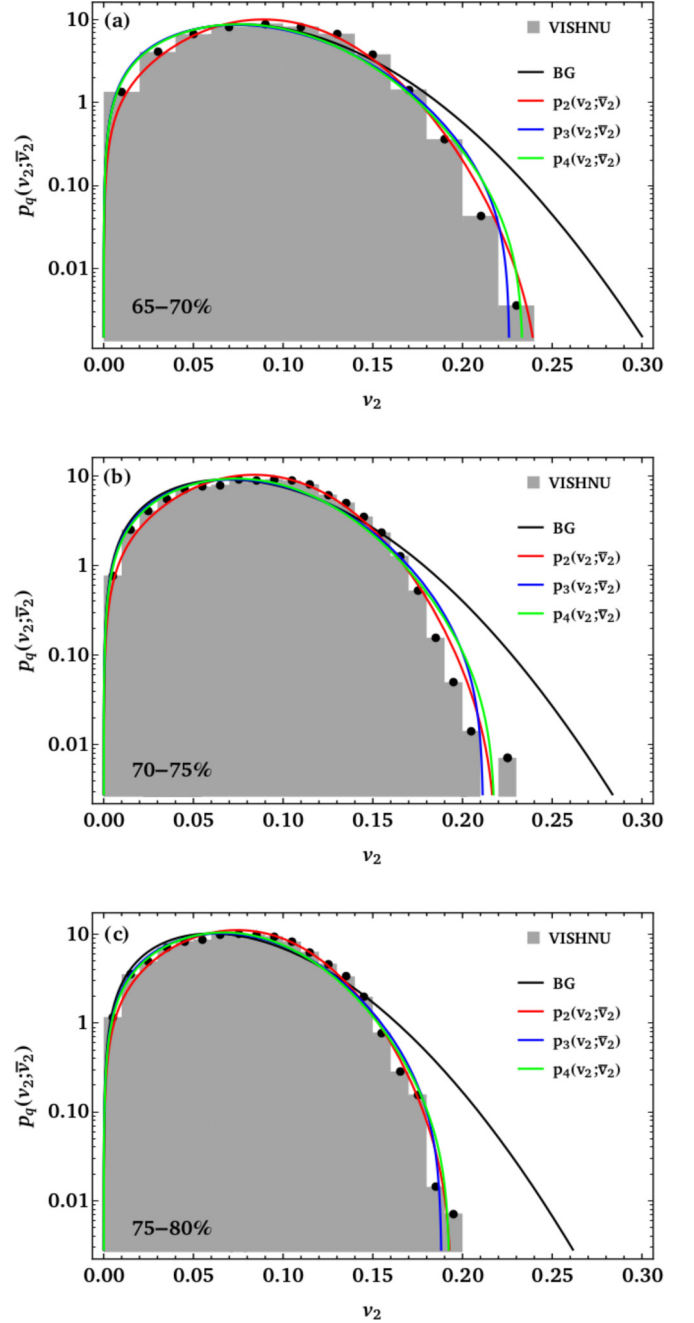


FIG. 3. Comparing the obtained flow distribution from iEBE-VISHNU output with different truncations of distribution $p_q(v_n; \bar{v}_n)$ for $q = 0, 2, 3, 4$ presented by dotted black, dashed red, dot-dashed blue, and solid green lines, respectively.

of elliptic flow is deviated from the Bessel-Gaussian distribution. So, the corrections to the Bessel-Gaussian distribution becomes important which is described by $p_q(v_n; \bar{v}_n)$.

IV. JOINT FLOW DISTRIBUTION

The information of the event-by-event flow fluctuations are encoded in the joint flow harmonic distribution $p(v_1, v_2, \dots)$, as mentioned in Sec. I. Therefore, using joint cumulant- and moment-generating functions, I obtain joint distribution of

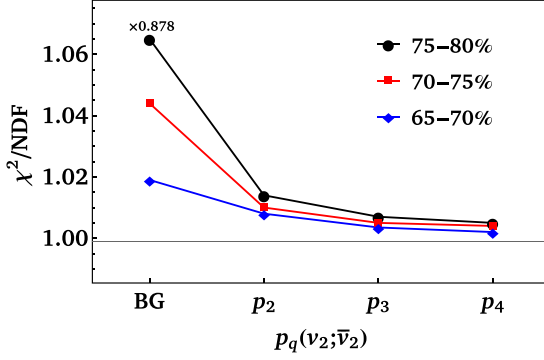


FIG. 4. χ^2/NDF values of fitting the Bessel-Gaussian distribution and $p_q(v_n; \bar{v}_n)$ for $q = 2, 3, 4$ to simulation plotted in 65–70%, 70–75%, and 75–80% centrality collisions. The corresponding χ^2/NDF value of the Bessel-Gaussian distribution multiplied by 0.878. This is done to increase the resolution in other parts of the plot.

flow harmonics in this section. To do this, I consider the relation between joint generating functions of moments and cumulants as follows:

$$\langle e^{W_n \lambda_n + W_m \lambda_m} \rangle = \exp \left[\sum_{k,l=0} \frac{(\lambda_n)^k (\lambda_m)^l}{k!l!} \mathcal{K}_{kl} \right], \quad (32)$$

where W_n and \mathcal{K}_{nm} are shifted flow vectors and joint flow cumulants, respectively. The relations between \mathcal{K}_{kl} and moments are

$$\mathcal{K}_{00} = \mathcal{K}_{10} = \mathcal{K}_{01} = 0, \quad (33a)$$

$$\mathcal{K}_{11} = \langle W_n W_m^* \rangle = \langle v_n v_m \cos(\Psi_1 - \Psi_2) \rangle - \bar{v}_n \bar{v}_m, \quad (33b)$$

$$\mathcal{K}_{20} = \langle |W_n|^2 \rangle = \langle v_n^2 \rangle - \bar{v}_n^2, \quad (33c)$$

$$\mathcal{K}_{02} = \langle |W_m|^2 \rangle = \langle v_m^2 \rangle - \bar{v}_m^2, \quad (33d)$$

$$\vdots \quad (33e)$$

Note that because the average of sifted flow vector ($\langle W_n \rangle$) is zero the cumulants \mathcal{K}_{10} and \mathcal{K}_{01} are zero for all harmonics. Using Eq. (22), one can rewrite the cumulants of flow joint distribution in terms of $j_n\{2k\}$ and flow correlations are as follows:

$$\mathcal{K}_{11} = \text{Re}[\langle V_n V_m^* \rangle] - \bar{v}_n \bar{v}_m, \quad (34a)$$

$$\mathcal{K}_{20} = j_n\{2\}, \quad (34b)$$

$$\mathcal{K}_{02} = j_m\{2\}, \quad (34c)$$

$$\vdots \quad (34d)$$

$$\begin{aligned} \exp(G(\lambda_n, \lambda_m)) &= \exp \left[\sum_{k+l \geq 3} \tilde{\mathcal{K}}_{kl} (\lambda_n)^k (\lambda_m)^l \right] \exp \left[\lambda_n^2 \tilde{\mathcal{K}}_{20} + \lambda_m^2 \tilde{\mathcal{K}}_{02} + \lambda_n \lambda_m \tilde{\mathcal{K}}_{11} \right] \\ &= \exp \left[\sum_{k+l \geq 3} \tilde{\mathcal{K}}_{kl} (\lambda_n)^k (\lambda_m)^l \right] \mathcal{N}(\lambda_n, \lambda_m). \end{aligned} \quad (35)$$

where the standard joint cumulants $\tilde{\mathcal{K}}_{mn}$ are $\mathcal{K}_{mn}/(m!n!)$. Applying Fourier transforming to both sides of Eq. (32), one gets

$$\int dW_n dW_m \mathcal{P}(W_n, W_m) e^{W_n \lambda_n + W_m \lambda_m} = \exp \left[\sum_{k+l \geq 3} \tilde{\mathcal{K}}_{kl} (\lambda_n)^k (\lambda_m)^l \right] \mathcal{N}(\lambda_n, \lambda_m), \quad (36)$$

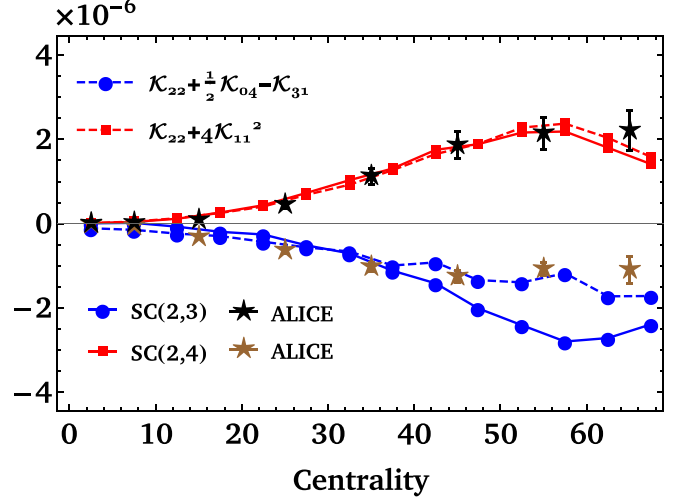


FIG. 5. Comparing the combinations of joint cumulants \mathcal{K} , $\mathcal{K}_{22} + \frac{1}{2}\mathcal{K}_{04} - \mathcal{K}_{31}$, and $\mathcal{K}_{22} + 4\mathcal{K}_{11}^2$ and symmetric cumulants obtained from iEBE-VISHNU with the results of ALICE Collaboration [8].

One way to investigate the event-by-event flow fluctuations is by measuring the correlation between the magnitudes of different flow harmonics using a cumulant analysis. These new observables are commonly known as *symmetric cumulants* (SC). Recently, ALICE has measured SC(2, 3) and SC(2, 4) as a function of centrality [8] at center-of-mass energy per nucleon pair $\sqrt{s} = 2.76$ TeV, with transverse momentum in the range of $0.2 < p_T < 5$ GeV. In this paper, I show that these experimental data can be explained by a combination of joint cumulants \mathcal{K} . Figure 5 present a comparison between simulation and experimental data. It is worth mentioning that using VISHNU output p_T is in the range $0.28 < p_T < 4$ GeV. As can be seen, there is a mismatch between SC(2, 3) obtained from simulation and experiment. But the experimental data can be described by combination $\mathcal{K}_{22} + \frac{1}{2}\mathcal{K}_{04} - \mathcal{K}_{31}$. Also, one can find that $\text{SC}(2, 4) = \mathcal{K}_{22} + 4\mathcal{K}_{11}^2$ can explain the ALICE data [39]. Now, having the joint cumulants enables us to obtain the joint distribution of flow harmonics. To do this, one should find a form of cumulative characteristic function $G(\lambda_n, \lambda_m)$ by expanding it to $k + l = 2$,

where $dW_n = dw_{n,x}dw_{n,y}$. Eventually, one finds the joint distribution $\mathcal{P}(W_n, W_m)$ as

$$\begin{aligned} \mathcal{P}(W_n, W_m) &= \frac{1}{2\pi\Delta} \exp\left[\sum_{k+l\geq 3} \tilde{\mathcal{K}}_{kl}(\partial_n)^k(\partial_m)^l\right] \exp\left[-\frac{\tilde{\mathcal{K}}_{02}w_n^2 + \tilde{\mathcal{K}}_{20}w_m^2 - \tilde{\mathcal{K}}_{11}(w_{n,x}w_{m,x} + w_{n,y}w_{m,y})}{\Delta^2}\right] \\ &\approx \left[1 + \sum_{k+l\geq 3} \tilde{\mathcal{K}}_{kl}(\partial_n)^k(\partial_m)^l\right] \mathcal{N}(W_n, W_m), \end{aligned} \quad (37)$$

where Δ defined $(4\tilde{\mathcal{K}}_{20}\tilde{\mathcal{K}}_{02} - \tilde{\mathcal{K}}_{11}^2)^{1/2}$ or in the simplified case $(j_n\{2\}j_m\{2\} - \text{Re}[\langle V_n V_m^* \rangle^2])^{1/2}$. Note that if one only considers $\mathcal{N}(W_n, W_m)$ as the first term of $\mathcal{P}(W_n, W_m)$ and compare it with bivariate normal distribution [40], then the following relations are obtained:

$$\sigma_n^2 = 2\tilde{\mathcal{K}}_{20} = \langle |W_n|^2 \rangle, \quad (38a)$$

$$\sigma_m^2 = 2\tilde{\mathcal{K}}_{20} = \langle |W_m|^2 \rangle, \quad (38b)$$

$$\rho_{nm} = \frac{\tilde{\mathcal{K}}_{11}}{2\sqrt{\tilde{\mathcal{K}}_{20}\tilde{\mathcal{K}}_{02}}} = \frac{\text{Re}[\langle W_n W_m^* \rangle]}{\sqrt{\langle |W_n|^2 \rangle \langle |W_m|^2 \rangle}}. \quad (38c)$$

These results show that the general joint distribution of flow vectors can be obtained,

$$\mathcal{P}(W_1, W_2, \dots, W_n) \approx \left[1 + \sum_{k_1+\dots+k_n\geq 3} \tilde{\mathcal{K}}_{k_1\dots k_n}(\partial_1)^{k_1} \dots (\partial_n)^{k_n}\right] \mathcal{N}(W_1, W_2, \dots, W_n), \quad (39)$$

by defining the joint cumulant- and moment-generating function relation,

$$\langle e^{W_1\lambda_1+\dots+W_n\lambda_n} \rangle = \exp\left[\sum_{k_1,\dots,k_n=0} \frac{(\lambda_1)^{k_1} \dots (\lambda_n)^{k_n}}{k_1! \dots k_n!} \mathcal{K}_{k_1\dots k_n}\right], \quad (40)$$

where $\mathcal{K}_{k_1\dots k_n}$ are the generalized joint cumulants, and the first cumulant, $\mathcal{K}_{0\dots 0}$, is equal to zero by considering the normalization condition of the probability distribution. Note that the distribution $\mathcal{N}(W_1, W_2, \dots, W_n)$ in Eq. (39) is a generalization of the one-dimensional normal distribution to higher dimensions which is dubbed as the joint normal distribution. But it should be noted that since the souls of the multivariate normal distribution and the distribution $\mathcal{N}(W_1, W_2, \dots, W_n)$ in Eq. (40) are different, one gets $\int dW_1 \dots dW_n \mathcal{N}(W_1, W_2, \dots, W_n) \neq 1$. So in the following, I use normalized kernel $\mathcal{N}(W_1, W_2, \dots, W_n)$ to find the joint distribution of flow magnitudes.

Let us return to the computation of the joint radial distribution of two flow harmonics using Eq. (37). In Ref. [41], a technique has been introduced that enables us to study the correlations between any rapidity windows and any harmonics. In this technique denoting the relative angle $\Phi = \Psi_m - \Psi_n$ [42], and averaging over reaction plane angle, the joint radial flow distribution is obtained as

$$\begin{aligned} &\int dv_n dv_m \mathcal{P}(v_n; \bar{v}_n, v_m; \bar{v}_m) \\ &= \int v_n dv_n v_m dv_m \int \frac{d\mathcal{P}(W_n, W_m)}{d\Psi_m d\Psi_n} d\Psi_m d\Psi_n d\Phi \\ &\quad \times \delta(\Phi - \Psi_m + \Psi_n). \end{aligned} \quad (41)$$

To study the joint radial flow distribution, I consider the first term in Eq. (37) for simplicity. Inserting it into Eq. (41) one

obtains the joint flow distribution [43]:

$$\begin{aligned} &\int dv_n dv_m \mathcal{P}_1(v_n; \bar{v}_n, v_m; \bar{v}_m) \\ &= \int dv_n dv_m d\Phi \chi_{mn} e^{\zeta_3 \cos \Phi} I_0[\sqrt{\zeta_1^2 + \zeta_2^2 + 2\zeta_1 \zeta_2 \cos(\Phi)}], \end{aligned} \quad (42)$$

where

$$\chi_{mn} \equiv \frac{4v_n v_m}{\pi \Delta^2} \exp\left[-\frac{v_n^2 + \bar{v}_n^2}{\Delta^2/2\tilde{\mathcal{K}}_{02}} - \frac{v_m^2 + \bar{v}_m^2}{\Delta^2/2\tilde{\mathcal{K}}_{20}} + \frac{\bar{v}_n \bar{v}_m}{\Delta^2/2\tilde{\mathcal{K}}_{11}}\right], \quad (43a)$$

$$\zeta_1 \equiv v_n \left(\frac{2\bar{v}_n}{\Delta^2/2\tilde{\mathcal{K}}_{02}} - \frac{\bar{v}_m}{\Delta^2/2\tilde{\mathcal{K}}_{11}}\right), \quad (43b)$$

$$\zeta_2 \equiv v_m \left(\frac{2\bar{v}_m}{\Delta^2/2\tilde{\mathcal{K}}_{20}} - \frac{\bar{v}_n}{\Delta^2/2\tilde{\mathcal{K}}_{11}}\right), \quad (43c)$$

$$\zeta_3 \equiv \frac{\bar{v}_n \bar{v}_m}{\Delta^2/2\tilde{\mathcal{K}}_{11}}. \quad (43d)$$

Note that Eq. (42) is the first approximation of the radial joint distribution of any two flow harmonics. To study the distribution $\mathcal{P}(v_n; \bar{v}_n, v_m; \bar{v}_m)$, I investigate it for v_2 and v_3 . In this case, since the triangular flow distribution is rotationally symmetric, \bar{v}_3 is zero. Also, as mentioned above, Δ_{v_2, v_3}^2 is $j_2\{2\}j_3\{2\} - \text{Re}[\langle V_2 V_3^* \rangle^2]$. Checking Δ_{v_2, v_3}^2 , one finds that the term $\text{Re}[\langle V_2 V_3^* \rangle^2]$ is very small and negligible against $j_2\{2\}j_3\{2\}$. So $\Delta_{v_2, v_3}^2 \simeq j_2\{2\}j_3\{2\}$ can be written. It should be noticed that the contribution of $\text{Re}[\langle V_2 V_3^* \rangle^2]$ in ζ_i is non-negligible, because it is in the numerator. Concerning these variables, the joint distribution of second and third harmonics

can be rewritten

$$\mathcal{P}_1(v_2; \bar{v}_2, v_3; 0) = \frac{4v_2v_3}{\pi j_2\{2\}j_3\{2\}} \exp\left[-\frac{v_2^2 + \bar{v}_2^2}{j_2\{2\}} - \frac{v_3^2}{j_3\{2\}}\right] \times \int d\Phi I_0[\sqrt{\gamma_1^2 + \gamma_2^2 + 2\gamma_1\gamma_2 \cos(\Phi)}], \quad (44)$$

where

$$\gamma_1 \equiv \frac{2v_n\bar{v}_n}{\mathcal{K}_{20}}, \quad \gamma_2 \equiv -\frac{v_n\bar{v}_n}{\mathcal{K}_{20}\mathcal{K}_{02}/2\mathcal{K}_{11}}. \quad (45)$$

Equation (44) shows that because there is a nonnegligible correlation between V_2 and V_3 the first approximation of joint distribution $\mathcal{P}(v_2; \bar{v}_2, v_3; 0)$ cannot be written as $p_0(v_3; 0)p_0(v_2; \bar{v}_2)$. Note that $p_0(v_n; \bar{v}_n)$ is the first truncation of the distribution Eq. (31) which is called the Bessel-Gaussian distribution. However, I checked that if one considers $\mathcal{P}(v_2; \bar{v}_2, v_3; 0) = p_0(v_3; 0)p_0(v_2; \bar{v}_2)$, its results and the results of Eq. (44) approximately are the same. Figure 6 present the smooth density histogram of v_2 and v_3 , which is obtained by using the results of the event-by-event 3 + 1D viscous hydrodynamics at center-of-mass energy per nucleon pair $\sqrt{s} = 5.02$ TeV [44]. These data are obtained with the wounded-quark initial conditions, and the contour plot of the first term of distribution $\mathcal{P}(v_2; \bar{v}_2, v_3; 0)$ in 30–40% centrality. As can be seen in this figure, the results show that there is a decent agreement between theory and simulation data. To find the best estimation, one have to insert the complete form of Eq. (37) in Eq. (41).

V. CONCLUSION

In this paper, I employed the relation between joint cumulant- and moment-generating function of $v_{n,x}$ and $v_{n,y}$ to relate the radial flow distribution to cumulants by using the standard method of finding Gram-Charlier series. I have found a general flow distribution in Eq. (31) by using Fourier transformation both sides of Eq. (21). It is an expansion around Bessel-Gaussian distribution where the coefficients of the expansion have been written in terms of shifted cumulants $j_n\{2k\}$. I have shown that $p(v_n; \bar{v}_n)$ can explain the generated data in the peripheral collisions, by assuming $\bar{v}_n \neq 0$ for even harmonics. My results indicate a significant improvement over the Bessel-Gaussian distribution. Also, I have obtained the odd flow distribution which has been found in Refs. [22] and [23] by setting $\bar{v}_n = 0$. The shifted cumulants $j_n\{2k\}$ were written in terms of moments $\langle w_n^k \rangle$ where w_n is the magnitude of the shifted flow vector. If one assumes $\bar{v}_n = 0$, then the cumulants $j_n\{2k\}$ would be 2k-particle correlation functions $c_n\{2k\}$ which can be observed experimentally. Also, I have shown that the shifted cumulants $j_n\{2k\}$, which is obtained from the relation between joint cumulant- and moment-generating functions, have more information than the cumulants q_n found in previous works. In the final step, I have studied the joint distribution of flow harmonics and presented a general form for $\mathcal{P}(W_1, W_2, \dots, W_n)$. To do this, I introduced new observables \mathcal{K}_{nm} and showed that the experimental data for symmetric cumulants SC(2, 3) and SC(2, 4) can be explained by combinations of these observables. So I think that the cumulants \mathcal{K}_{nm} can be interesting observables for

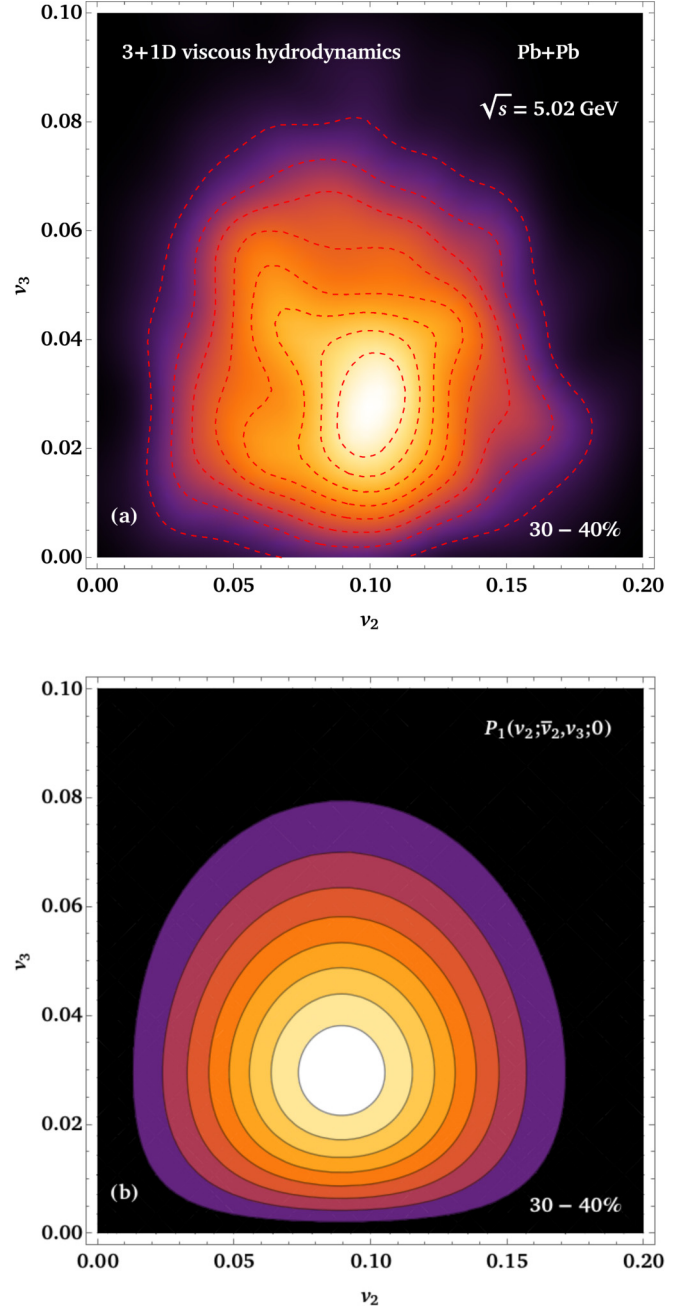


FIG. 6. Comparing the smooth density histogram of v_2 and v_3 obtained from 3 + 1D viscous hydrodynamic simulation [44] and the contour plot of the first term of distribution $\mathcal{P}(v_2; \bar{v}_2, v_3; 0)$ in 30–40% centrality class.

experimentalists. I also obtained the joint radial distribution of the two flow harmonics and showed that the first terms of this distribution for v_2 and v_3 can justify the simulation data. Investigating joint distributions of other flow harmonics is left to future studies.

ACKNOWLEDGMENTS

I thank Jean-Yves Ollitrault and Fatemeh Elahi for useful discussions and comments, as well as Hessamadin Arfaei for all his supports. This research is supported by the Institute for Research in Fundamental Sciences (IPM).

APPENDIX A: ODD FLOW DISTRIBUTION

As mentioned in Sec. II, in Eq. (8) only terms with $k = l$ are nonzero. Moreover, Eq. (8) can be written as

$$G(\lambda_x, \lambda_y) = \langle e^{v_{n,x}\lambda_x + v_{n,y}\lambda_y} \rangle \exp \left[\sum_{k=1}^{\infty} \frac{(\lambda_x^2 + \lambda_y^2)^k}{2^{(2k)}(k!)^2} c_n\{2k\} \right]. \quad (\text{A1})$$

Since I use the Gram-Charlier series with normal kernel, I can rewrite $G(\lambda_x, \lambda_y)$ as follows:

$$G(\lambda_x, \lambda_y) = \exp \left[\sum_{k=2}^{\infty} \frac{(\lambda_x^2 + \lambda_y^2)^k}{2^{(2k)}(k!)^2} c_n\{2k\} \right] e^{\frac{\lambda_x^2 + \lambda_y^2}{4} c_n\{2\}}. \quad (\text{A2})$$

One can find the odd flow distribution $p_{\text{odd}}(v_{n,x}, v_{n,y})$ by using inverse Fourier transform of $G(\lambda_x, \lambda_y)$,

$$\begin{aligned} p_{\text{odd}}(v_{n,x}, v_{n,y}) &= \frac{1}{(2\pi)^2} \int_{-\infty}^{\infty} \int_{-\infty}^{\infty} d\lambda_x d\lambda_y e^{-i(v_{n,x}\lambda_x + v_{n,y}\lambda_y)} G(\lambda_x, \lambda_y) \\ &= \frac{1}{(2\pi)^2} \int_{-\infty}^{\infty} \int_{-\infty}^{\infty} d\lambda_x d\lambda_y e^{-i(v_{n,x}\lambda_x + v_{n,y}\lambda_y)} \exp \left[\sum_{k=2}^{\infty} \frac{((-i\lambda_x)^2 + (-i\lambda_y)^2)^k}{2^{(2k)}(k!)^2} c_n\{2k\} \right] e^{-\frac{\lambda_x^2 + \lambda_y^2}{4} c_n\{2\}}. \end{aligned} \quad (\text{A3})$$

Since I also mentioned that $(it)^n G_N(t)$ is the characteristic function of $(-D)^n G_N(x)$, the following relation is obtained:

$$\begin{aligned} p_{\text{odd}}(v_{n,x}, v_{n,y}) &= \frac{1}{(2\pi)^2} \exp \left[\sum_{k=2}^{\infty} \frac{(\partial_x^2 + \partial_y^2)^k}{2^{(2k)}(k!)^2} c_n\{2k\} \right] \int_{-\infty}^{\infty} \int_{-\infty}^{\infty} d\lambda_x d\lambda_y e^{-i(v_{n,x}\lambda_x + v_{n,y}\lambda_y)} e^{-\frac{\lambda_x^2 + \lambda_y^2}{4} c_n\{2\}} \\ &= \frac{1}{(2\pi)^2} \exp \left[\sum_{k=2}^{\infty} \frac{(\partial_x^2 + \partial_y^2)^k}{2^{(2k)}(k!)^2} c_n\{2k\} \right] \left[\frac{4\pi}{c_n\{2\}} e^{-\frac{v_{n,x}^2 + v_{n,y}^2}{c_n\{2\}}} \right] \\ &= \exp \left[\sum_{k=2}^{\infty} \frac{c_n\{2k\}(\partial_x^2 + \partial_y^2)^k}{2^{2k}(k!)^2} \right] \left[\frac{1}{\pi c_n\{2\}} e^{-\frac{v_{n,x}^2 + v_{n,y}^2}{c_n\{2\}}} \right]. \end{aligned} \quad (\text{A4})$$

APPENDIX B: GENERAL FORM OF RADIAL DERIVATIVES

If one differentiates 1D normal distribution, $\mathcal{N}(r) = e^{-\frac{r^2}{a}} / (\sqrt{\pi a})$ with $a = 2\sigma^2$, n times, then the result of each time is approximately a Laguerre polynomial,

$$\begin{aligned} k = 1 : D_r^1 \mathcal{N}(r) &= D_r \left(\mathcal{N}(r) L_0 \left(\frac{r^2}{a} \right) \right), \\ k = 2 : D_r^2 \mathcal{N}(r) &\approx D_r \left(\mathcal{N}(r) L_1 \left(\frac{r^2}{a} \right) \right), \\ k = 3 : D_r^3 \mathcal{N}(r) &\approx D_r \left(\mathcal{N}(r) L_2 \left(\frac{r^2}{a} \right) \right), \\ k = 4 : D_r^4 \mathcal{N}(r) &\approx D_r \left(\mathcal{N}(r) L_3 \left(\frac{r^2}{a} \right) \right), \\ &\vdots \\ k = n : D_r^n (e^{-\frac{r^2}{a}}) &\approx D_r \left(\mathcal{N}(r) L_n \left(\frac{r^2}{a} \right) \right). \end{aligned} \quad (\text{B1})$$

Note that the radial derivative is $D_r = \partial_r^2 + (1/r)\partial_r$. Using above derivative in Eq. (17), one can rewrite the $p(v_n)$ as follows:

$$p_{\text{odd}}(v_n) = \frac{2v_n}{c_n\{2\}} \left\{ e^{-\frac{v_n^2}{c_n\{2\}}} + \sum_{k=2}^{\infty} \frac{c_n\{2k\}}{4^k (k!)^2} \left[\left(-\frac{4}{c_n\{2\}} \right)^{k-1} (k-1)! \right] D_{v_n} \left[e^{-\frac{v_n^2}{c_n\{2\}}} L_{k-1} \left(\frac{v_n^2}{c_n\{2\}} \right) \right] \right\}. \quad (\text{B2})$$

If one differentiates $\mathcal{N}(r) L_{k-1}(\frac{r^2}{a})$ in the radial direction,

$$D_r \left(\mathcal{N}(r) L_{k-1} \left(\frac{r^2}{a} \right) \right) = -\frac{4n}{a} \mathcal{N}(r) L_k \left(\frac{r^2}{a} \right), \quad (\text{B3})$$

and then replace it in Eq. (B2), in the result one obtains the distribution of odd flow harmonics as

$$p_{\text{odd}}(v_n) = \left(\frac{2v_n}{c_n\{2\}} \right) e^{-\frac{v_n^2}{c_n\{2\}}} \left[1 + \sum_{k=2} \frac{(-1)^k c_n\{2k\}}{k! c_n\{2\}^k} L_k(v_n^2/c_n\{2\}) \right]. \quad (\text{B4})$$

APPENDIX C: TWO-DIMENSIONAL DERIVATIVES

As mentioned in Sec. III, to find a general flow distribution one gets

$$p(v_{n,x}, v_{n,y}) = \exp \left[\sum_{k=2} \frac{j_n\{2k\} D^k}{4^k (k!)^2} \right] \mathcal{F}(v_{n,x}, v_{n,y}), \quad (\text{C1})$$

by using Eq. (21) and considering the relation

$$\int D\lambda (\lambda_x^2 + \lambda_y^2)^k e^{-i(v_{n,x} - \bar{v}_n)\lambda_x - i v_{n,y}\lambda_y} \times e^{-(\lambda_x^2 + \lambda_y^2)j_n\{2\}/4} = D^k \int D\lambda e^{-i(v_{n,x} - \bar{v}_n)\lambda_x - i v_{n,y}\lambda_y} \times e^{-(\lambda_x^2 + \lambda_y^2)j_n\{2\}/4}, \quad (\text{C2})$$

where $D\lambda = d\lambda_x d\lambda_y$. Evaluating the derivative D for $k = 1, 2, \dots, k$ in Eq. (C1), one obtains:

$$\begin{aligned} k = 1 : D^1 \mathcal{F}(v_{n,x}, v_{n,y}) &= -\frac{4}{j_n\{2\}} \mathcal{F}(v_{n,x}, v_{n,y}) L_1 \left[\frac{(v_{n,x} - \bar{v}_n)^2 + v_{n,y}^2}{j_n\{2\}} \right], \\ &\vdots \\ k = n : D^n \mathcal{F}(v_{n,x}, v_{n,y}) &= \frac{(-1)^n 4^n n!}{j_n\{2\}^n} \mathcal{F}(v_{n,x}, v_{n,y}) L_n \left[\frac{(v_{n,x} - \bar{v}_n)^2 + v_{n,y}^2}{j_n\{2\}} \right]. \end{aligned} \quad (\text{C3})$$

Note that the calculations of Eq. (C3) are obtained by using Cartesian partial derivatives. To find radial flow distribution one has to integrate over azimuthal angle. Therefore, it is better to write down in polar coordinates,

$$\begin{aligned} k = 1 : D_{v_n, \Psi_n}^1 \mathcal{F}(v_n; \bar{v}_n, \Psi_n) &= -\frac{4}{a} \mathcal{F}(v_n; \bar{v}_n, \Psi_n) \left[L_1 \left(\frac{v_n^2 + \bar{v}_n^2}{j_n\{2\}} \right) + A_1 + B_1 \right], \\ &\vdots \\ k = n : D_{v_n, \Psi_n}^n \mathcal{F}(v_n; \bar{v}_n, \Psi_n) &= \frac{(-1)^n 4^n n!}{a^n} \mathcal{F}(v_n; \bar{v}_n, \Psi_n) \left[L_n \left(\frac{v_n^2 + \bar{v}_n^2}{j_n\{2\}} \right) + A_n + B_n \right], \end{aligned} \quad (\text{C4})$$

where A_k and B_k are

$$\begin{aligned} A_1 &= 0, \\ B_1 &= \frac{2v_n \bar{v}_n}{j_n\{2\}} \cos \Psi_n, \\ A_2 &= \frac{v_n^2 \bar{v}_n^2}{j_n\{2\}^2}, \\ B_2 &= \frac{2v_n \bar{v}_n}{j_n\{2\}} \left[2L_1 \left(\frac{v_n^2 + \bar{v}_n^2}{2j_n\{2\}} \right) \right] \cos \Psi_n + \frac{v_n^2 \bar{v}_n^2}{j_n\{2\}^2} \cos 2\Psi_n, \\ A_3 &= \frac{v_n^2 \bar{v}_n^2}{j_n\{2\}^2} \left[3L_1 \left(\frac{v_n^2 + \bar{v}_n^2}{3j_n\{2\}} \right) \right], \\ B_3 &= \frac{2v_n \bar{v}_n}{j_n\{2\}} \left[3L_2 \left(\frac{v_n^2 + \bar{v}_n^2}{2j_n\{2\}} \right) + \frac{1}{8j_n\{2\}^2} (v_n^4 + 6v_n^2 \bar{v}_n^2 + \bar{v}_n^4) \right] \cos \Psi_n + \frac{v_n^2 \bar{v}_n^2}{j_n\{2\}^2} \left[3L_1 \left(\frac{v_n^2 + \bar{v}_n^2}{3j_n\{2\}} \right) \right] \cos 2\Psi_n + \frac{v_n^3 \bar{v}_n^3}{3j_n\{2\}^3} \cos 3\Psi_n, \\ &\vdots \\ A_k &= \alpha_k, \\ B_k &= \sum_{l=1}^k \beta_{kl} \cos l\Psi_n. \end{aligned} \quad (\text{C5})$$

- [1] K. H. Ackermann *et al.* (STAR Collaboration), *Phys. Rev. Lett.* **86**, 402 (2001).
- [2] R. A. Lacey (PHENIX Collaboration), *Nucl. Phys. A* **698**, 559 (2002).
- [3] I. C. Park *et al.* (PHOBOS Collaboration), *Nucl. Phys. A* **698**, 564 (2002).
- [4] K. Aamodt *et al.* (ALICE Collaboration), *Phys. Rev. Lett.* **105**, 252302 (2010).
- [5] K. Aamodt *et al.* (ALICE Collaboration), *Phys. Rev. Lett.* **107**, 032301 (2011).
- [6] S. Chatrchyan *et al.* (CMS Collaboration), *Phys. Rev. C* **87**, 014902 (2013).
- [7] G. Aad *et al.* (ATLAS Collaboration), *Phys. Lett. B* **707**, 330 (2012).
- [8] G. Aad *et al.* (ATLAS Collaboration), *Eur. Phys. J. C* **74**, 3157 (2014).
- [9] A. M. Poskanzer and S. A. Voloshin, *Phys. Rev. C* **58**, 1671 (1998).
- [10] R. S. Bhalerao, N. Borghini, and J. Y. Ollitrault, *Phys. Lett. B* **580**, 157 (2004).
- [11] R. S. Bhalerao, N. Borghini, and J. Y. Ollitrault, *Nucl. Phys. A* **727**, 373 (2003).
- [12] N. Borghini, P. M. Dinh, and J. Y. Ollitrault, *Phys. Rev. C* **63**, 054906 (2001).
- [13] N. Borghini, P. M. Dinh, and J. Y. Ollitrault, *Phys. Rev. C* **64**, 054901 (2001).
- [14] S. S. Adler *et al.* (PHENIX Collaboration), *Phys. Rev. C* **77**, 014905 (2008).
- [15] K. Aamodt *et al.* (ALICE Collaboration), *Phys. Rev. Lett.* **106**, 032301 (2011).
- [16] B. Schenke, P. Tribedy, and R. Venugopalan, *Phys. Rev. Lett.* **108**, 252301 (2012).
- [17] M. Miller and R. Snellings, [arXiv:nucl-ex/0312008](https://arxiv.org/abs/nucl-ex/0312008).
- [18] J. Jia and S. Mohapatra, *Phys. Rev. C* **88**, 014907 (2013).
- [19] G. Aad *et al.* (ATLAS), *J. High Energy Phys.* **11** (2013) 183.
- [20] S. A. Voloshin, [arXiv:nucl-th/0606022](https://arxiv.org/abs/nucl-th/0606022).
- [21] S. A. Voloshin, A. M. Poskanzer, A. Tang, and G. Wang, *Phys. Lett. B* **659**, 537 (2008).
- [22] N. Abbasi, D. Allahbakhshi, A. Davody, and S. F. Taghavi, *Phys. Rev. C* **98**, 024906 (2018).
- [23] H. Mehrabpour and S. F. Taghavi, *Eur. Phys. J. C* **79**, 88 (2019).
- [24] C. Shen, Z. Qiu, H. Song, J. Bernhard, S. Bass, and U. Heinz, *Comput. Phys. Commun.* **199**, 61 (2016).
- [25] J. Adam *et al.* (ALICE Collaboration), *Phys. Rev. Lett.* **117**, 182301 (2016).
- [26] J. Jia (ATLAS Collaboration), *Nucl. Phys. A* **910–911**, 276 (2013).
- [27] G. Aad *et al.* (ATLAS Collaboration), *Phys. Rev. C* **90**, 024905 (2014).
- [28] M. G. Kendall, *The Advanced Theory of Statistics* (Charles Griffin and Company, London, 1945).
- [29] H. Cramer, *Mathematical Methods of Statistics*, Princeton Mathematical Series Vol. 9 (Princeton University Press, Princeton, NJ, 1946).
- [30] W. Krzanowski, *Principles of Multivariate Analysis*, Oxford Statistical Science Series (Oxford University Press, Oxford, 2000).
- [31] Consider a function $p(x)$ with Fourier transform $G(t)$ such that

$$p(x) = \frac{1}{2\pi} \int_{-\infty}^{\infty} G(t) e^{-itx} dt.$$

To find the Fourier transform of $dp(x)/dx$, a simple way, using the antitransform:

$$\frac{dp(x)}{dx} = \frac{d}{dx} \left(\frac{1}{2\pi} \int_{-\infty}^{\infty} G(t) e^{-itx} dt \right) = \frac{1}{2\pi} \int_{-\infty}^{\infty} (-it) G(t) e^{-itx} dt.$$

Hence, the Fourier transform $dp(x)/dx$ is $(-it)G(t)$.

- [32] T. Brenn and S. N. Anfinson, A revisit of the Gram-Charlier and Edgeworth series expansions, UiT The Arctic University of Norway, Department of Physics and Technology, Tech. Rep., June 2017, <https://munin.uit.no/bitstream/handle/10037/11261/article.pdf?isAllowed=y&sequence=1>.
- [33] G. A. Young, M2S1 Lecture Notes, September 2009, <http://wwwf.imperial.ac.uk/~ayoung/m2s1/M2S12009.pdf>.
- [34] Note that to find the averaged flow magnitude one has to integrate the generating moments over ϕ_λ in polar coordinates

$$G(\lambda) = \frac{1}{2\pi} \int_0^{2\pi} d\phi_\lambda \langle e^{\lambda \cdot v} \rangle,$$

where $\lambda_x = \lambda \cos \phi_\lambda$ and $\lambda_y = \lambda \sin \phi_\lambda$.

- [35] Note that $\langle v_{n,x} \rangle$ is zero for the odd flow distribution.
- [36] In the integration I use $\lambda_x \rightarrow -i\lambda_x$ and $\lambda_y \rightarrow -i\lambda_y$.
- [37] It is well-known that the averaged ellipticity $\tilde{v}_2 \equiv \langle v_{2,x} \rangle$ is a manifestation of the geometrical initial ellipticity for events in a given centrality class irrespective of the fluctuations. In general, one is able to define averaged flow harmonic $\tilde{v}_n \equiv \langle v_{n,x} \rangle$. Also, the average of $v_{n,y}$ is zero, $\langle v_{n,y} \rangle = 0$, because the distribution of $v_{n,y}$ is centered at 0 due to parity conservation and symmetry with respect to the reaction plane [45]. Moreover, I defined z with the shifted flow vector $W_n = (v_{v,x} - \tilde{v}_n) + iv_{n,y}$.
- [38] A flow distribution that works for even harmonics is a general distribution that is true for all harmonics. Furthermore, I use the notation $p(v_{n,x}, v_{n,y})$ instead of $p_{\text{even}}(v_{n,x}, v_{n,y})$ for nonrotational symmetric flow distribution.
- [39] In Ref. [46], authors have compared SC(2, 3) and SC(2, 4) obtained from iEBE-VISHNU in three different transverse momentum ranges with the experimental results from ALICE (see Fig. 12 in Ref. [33]). They have found that SC(2, 3) and SC(2, 4) obtained from ALICE data can be explained by SC(2, 3) and SC(2, 4) obtained from iEBE-VISHNU in different p_T ranges. Instead, I have kept p_T range the same and tried to find the combinations of \mathcal{K}_{mn} to explain the experimental results in a transverse momentum range.
- [40] In 2D, the probability density function of a vector $[x'y']$ is

$$f(x', y') = \frac{1}{2\pi\sigma_m\sigma_n\sqrt{1-\rho^2}} \times \exp\left(-\frac{1}{2(1-\rho^2)}\left[\frac{x'^2}{\sigma_x^2} + \frac{y'^2}{\sigma_y^2} - \frac{2\rho x'y'}{\sigma_x\sigma_y}\right]\right).$$

where σ and ρ are the standard deviation and the Pearson correlation, respectively.

- [41] S. Voloshin and Y. Zhang, *Z. Phys. C* **70**, 665 (1996).
- [42] Note that the angles Φ and Ψ are in the range of $[0, \pi]$ and $[0, 2\pi]$, respectively.
- [43] Here to normalize distribution $\mathcal{N}(W_n, W_m)$, I assume $\Delta \rightarrow \Delta/\sqrt{2}$.
- [44] P. Bozek, *Phys. Rev. C* **81**, 034909 (2010).
- [45] G. Giacalone, L. Yan, J. Noronha-Hostler, and J. Y. Ollitrault, *Phys. Rev. C* **95**, 014913 (2017).
- [46] C. Mordasini, A. Bilandzic, D. Karakoç, and S. F. Taghavi, *Phys. Rev. C* **102**, 024907 (2020).